Introduction to air-water flows 1

HELMUT KOBUS
Institut für Wasserbau, Universität Stuttgart, Germany

1.1 GENERAL TYPES OF AIR-WATER FLOWS

For many hydraulic structures, safe operation can only be achieved if not only the characteristics of the water flow are considered, but due attention is also given to the simultaneous movement of air in the system. Although the difference in specific weight of air and water is so large that they are usually well separated by a sharp interface, a number of flow configurations lead to an intensive mixing across this surface. This process is called air entrainment. Consideration of the effects of entrained air upon water flow may be essential to provide for the safe operation of a hydraulic structure.

Air flow can affect water flow in a great variety of flow configurations. We can distinugish the following categories:

1.1.1 *Air demand in hydraulic structures without mixing*

In order to maintain moderate pressures in closed hydraulic systems, air is often allowed to enter the system, and where it accumulates it is released from the system. Basically two configurations occur:

– Air flow to a finite-volume air chamber due to a falling or rising water surface affecting the chamber volume. For the design of adequate aeration devices, the resulting air demand can usually be computed in a straightforward manner.

– Air demand in closed conduits flowing partially full. The drag of the moving water surface generates an air flow which has to be accounted for at the intake (often requiring air vents) and at the outlet. The air demand can usually be estimated if the velocity of the water is known.

1.1.2 *Air entrainment in hydraulic structures (air demand with mixing)*

The complex two-phase flow resulting from the entrainment and transport of air

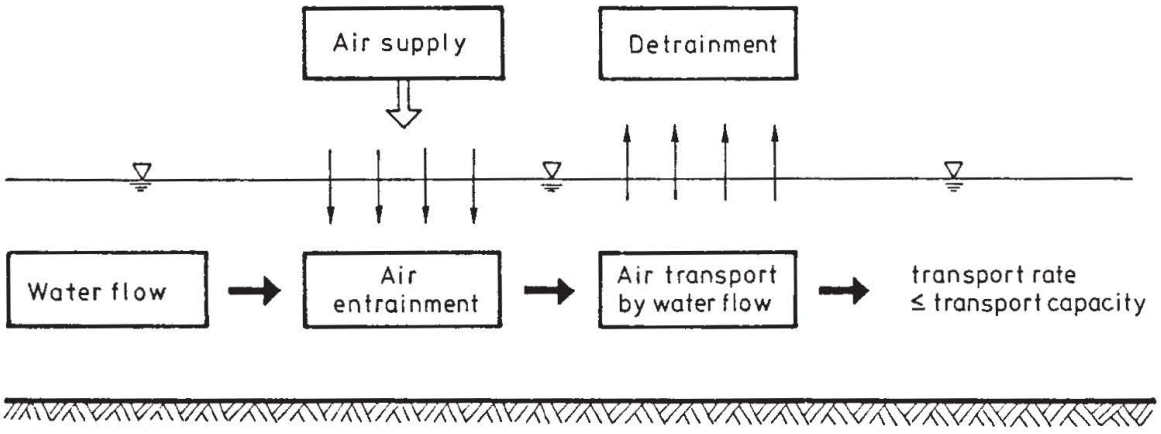

Figure 1.1. Air entrainment, detrainment and transport

bubbles is the subject of this monograph. The process which forces air through a surface into a water volume is called entrainment; the process of bubble escape from the surface is called detrainment. Many flow situations result in entrainment. The supply of air may be

– unlimited (air supply from the atmosphere); or

– limited as from an air chamber, which may or may not be connected to the atmosphere by an air duct. In this case an interaction occurs among air flow, water flow and air pressure in the system.

The region of detrainment is not necessarily near the region of entrainment; depending upon the water flow conditions and their transport capacity, the air may be transported over large distances to the region of detrainment (Figure 1.1). Here also one has to distinguish:

– unlimited air escape to the atmosphere;

– limited air escape in closed systems, leading to air accumulations in certain regions such as high points or along the top of conduits. These air pockets can impede the flow of water and thus have an undesirable effect upon it.

The major flow configurations leading to air entrainment in hydraulic structures are described in more detail in Section 1.2.

1.1.3 *Formation of air-water mixtures by air coming out of solution*

The saturation concentration for dissolved oxygen and nitrogen in water varies considerably with the pressure and the temperature of the water. Therefore, in closed-conduit systems changes in pressure and/or temperature can cause formation of small gas bubbles in the interior of the liquid. The elastic properties and the speed of wave propagation vary dramatically with the presence of gas bubbles even at very low concentrations. This phenomenon is important in the design of closed conduit systems, particularly with respect to fast changes in flow (hydrau-

lic transients). These phenomena are to be treated in the monograph *Air-water flow in closed conduits.*

1.1.4 *Designed aeration systems*

Designed aeration systems of various kinds are employed mainly for the reoxygenation of polluted water. They are primarily installed in sewage treatment plants and in polluted rivers and lakes for water quality enhancement. The various technical devices operate essentially on one of two principles:

– Formation of an air-water mixture at a surface: surface rotors, spray devices or water jet pumps supply either external energy or use part of the flow energy (thus contributing a considerable local energy gain or loss, respectively) in order to force air into the water.

– Formation of an air-water mixture by injecting air beneath the surface: submerged nozzles, perforated tubes or porous filter plates are employed for the dispersion of compressed air in the water. In sewage treatment, the injected air serves the dual purpose of providing oxygen to the water and, by the action of the bubbles, inducing both a water flow and increased mixing. Similar systems are employed in natural rivers and lakes as active means of improving the water quality. Bubble plumes and curtains also find applications as pneumatic oil barriers, vertical mixers for density currents, devices for combatting formation of an ice cover, damping underwater detonation waves, etc. A detailed treatment including design information for such systems is given elsewhere (Kobus, 1973).

1.2 TYPES OF AERATION AND PROCESSES OF ENTRAINMENT IN HYDRAULIC STRUCTURES

Flow conditions which cause air entrainment, i.e. transport of air through a free water surface, are termed *self-aerating*. They give rise to *surface aeration*, or else *natural aeration*. In some flows entrainment takes place all along the water surface (*ambient aeration*) and in others entrainment occurs locally at a surface discontinuity (*local aeration*). The following processes can be distinguished:

1.2.1 *Surface aeration in high-speed flows*

In high-speed open channel flows like those in spillways or chutes, the flow turbulence gives rise to surface disturbances which lead to air entrainment. Similarly, high-speed free jets generated by fire monitors, hollow jet valves, flip bucket ejectors, etc. experience surface disturbances due to the initial jet flow turbulence and to the shear forces of the surrounding air. These disturbances grow and lead to air entrainment along the jet surface and in many cases to a complete disintegration of the jet.

Figure 1.2. Surface aeration in high-speed flow (Surface of the air entraining region on Aviemore Spillway. Photo: P. Cain, 1978)

Figure 1.2 is a photograph of the surface of water flowing down a spillway at high speed. The effects of a multitude of irregular high-energy vortices result in a contorted three dimensional free surface. Through this surface, air is continually escaping and being trapped. The major entraining mechanisms are overturning surface waves and water droplets being projected above the water surface and then falling back. In penetrating the water surface, the droplets drag air into the water. This process was suggested by Lane (1939), Rajaratnam (1962) and Hino (1961). It has been demonstrated in some classic experiments by Volkart (1980). Also the mechanism of air entrapment in vortices as described below undoubtedly also contributes to entrainment. The mixing zone of air and water grows into the water region and may extend to the channel bottom.

1.2.2 *Local aeration by impinging jets*

Free-surface flow configurations leading to local air entrainment are always connected with some form of surface discontinuity. Several jet-type flow configurations are sketched in Figure 1.3. These include sharp-crested weirs, free overfalls and drop structures. These flows differ from ambient surface aeration in that the local aeration processes entrain air at a rate completely independent of the

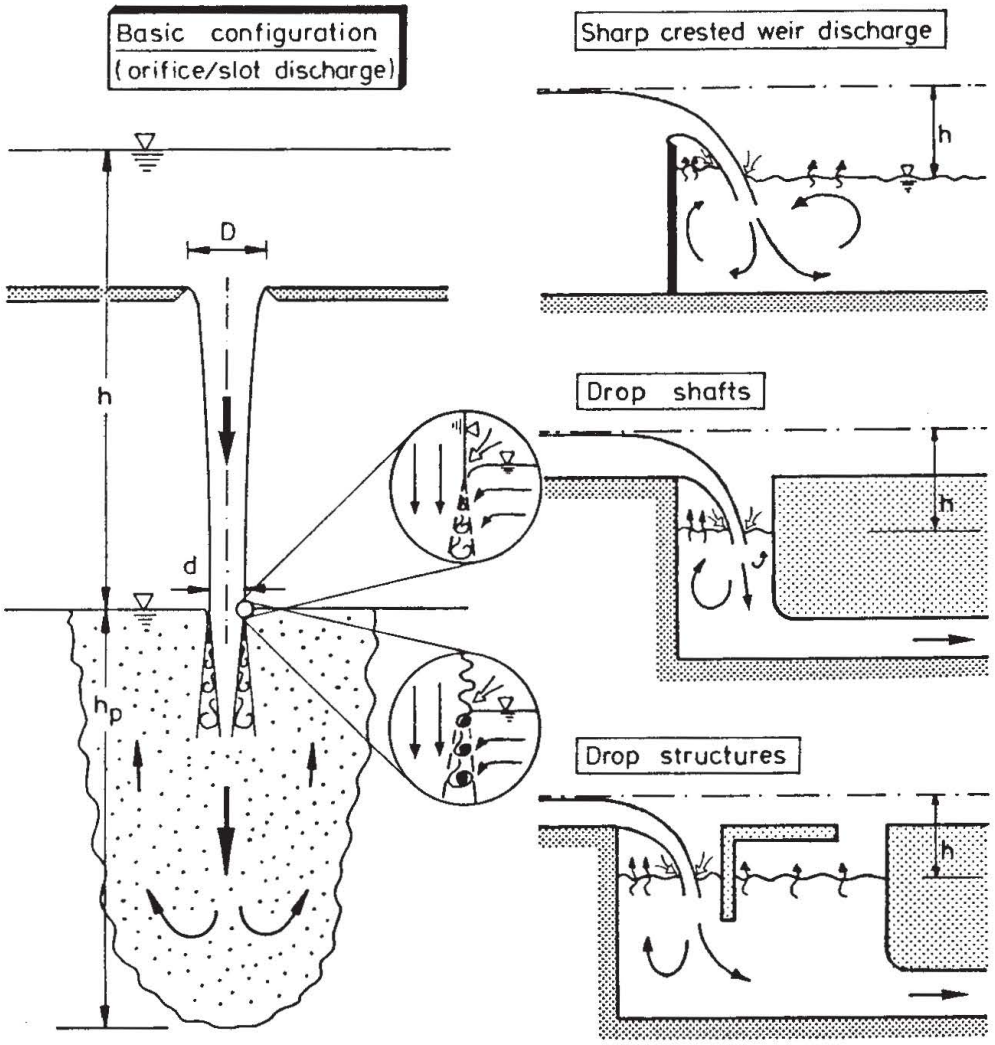

Figure 1.3. Local air entrainment at *plunging-jet type* configurations

transport capacity of the flow. The transport capacity only determines the distance over which the suspended air is transported. Thus, if the transport capacity of the flow is low, the entrained air will escape rather quickly, and the process of self-aeration will be important only locally. An example of this local aeration process is shown in Figure 1.4. The air bubbles entrained by the plunging free jet (upper left) escape from the stilling basin before the flow enters the subsequent duct (lower right).

Flow configurations with plunging jets are characterized by the fact that air entrainment takes place locally at the intersection of the free jet with the water surface. The momentum of the water jet causes air to be entrained in the highly turbulent shear layer induced by the jet surface. Figure 1.5 illustrates that the entrainment takes place mainly in relatively distinct vortices with longitudinal axes nominally perpendicular to the flow direction. Thomas (1978) suggested that the vortices in the intensive shear layer at the penetration point are sufficiently

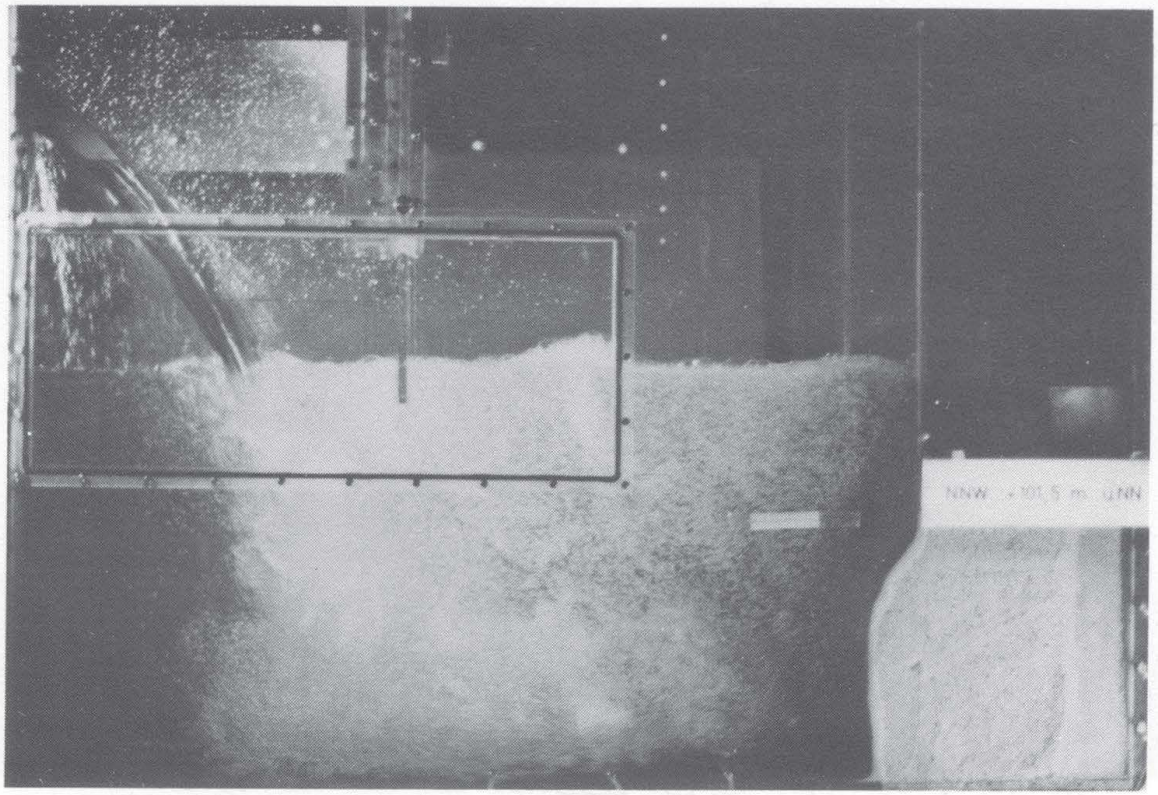

Figure 1.4. Air entrainment in a plunging free jet

strong to entrain air in the vortex cores. This type of entrainment may be enhanced by the development of turbulence on the jet surface prior to its contact with the free water surface (Ervine, 1976) and/or by the formation of a foam layer there.

The momentum flux of a plunging jet is predominantly vertical and downward. The vertical momentum flux component will be directly counteracted by the buoyancy of the entrained air. On the other hand the horizontal momentum flux components will remain essentially unchanged, since they experience no external force.

1.2.3 *Local aeration in hydraulic jump configurations*

Another surface- and velocity discontinuity causing air entrainment occurs at the toe of a hydraulic jump. Figure 1.7 shows that the local air entrainment at the toe of the surface roller occurs in much the same manner as in the plunging jet. Again, the air is entrained into the free shear layer which is characterized by intensive turbulence production, predominantly in vortices with axes perpendicular to the flow.

Stationary jumps are typically encountered downstream of control structures and in stilling basins, and related configurations are moving hydraulic jumps (surge waves) and the unsteady breaking of shallow water waves. Also, jets

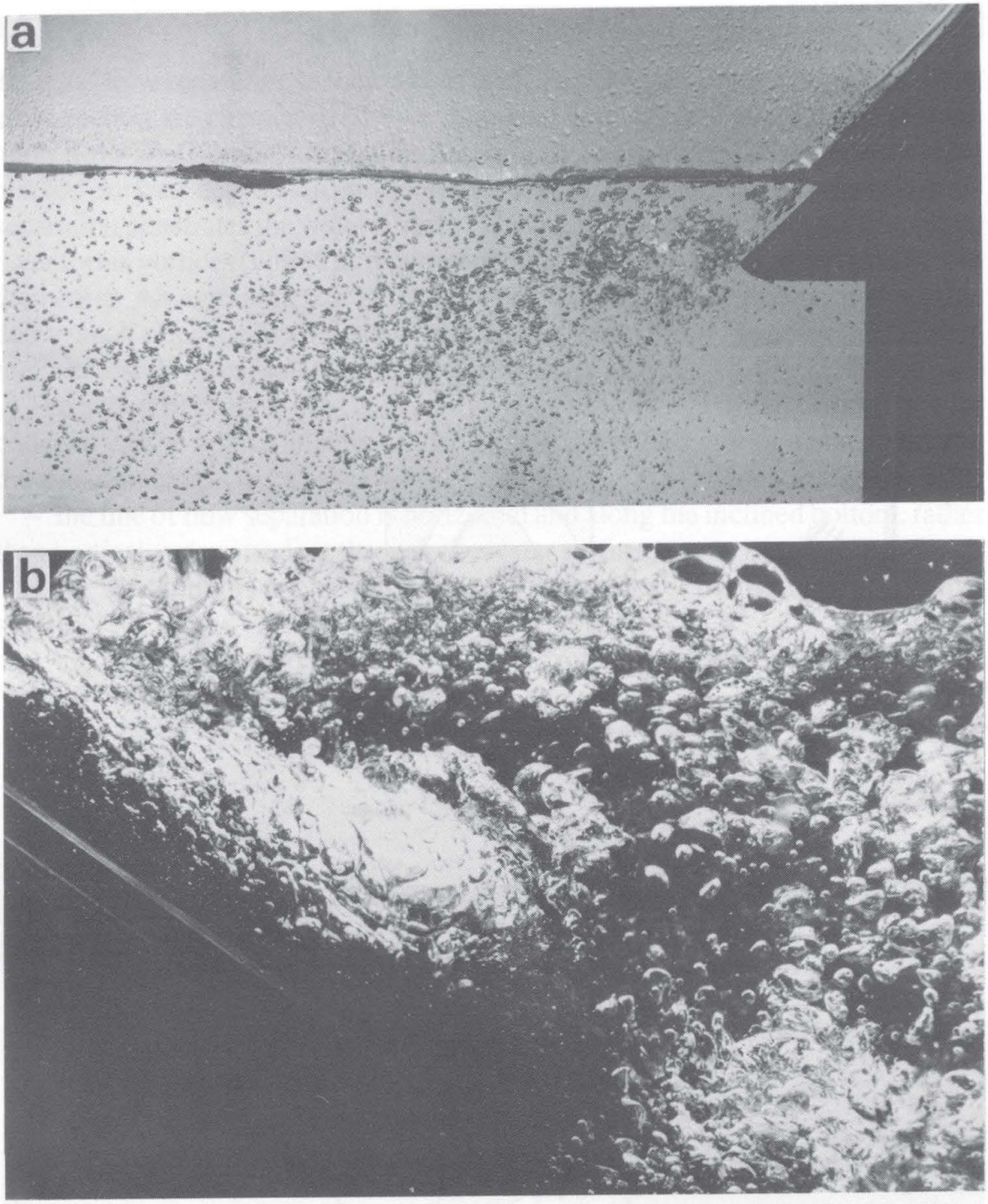

Figure 1.5. Air entrainment in a supported inclined jet caused by vortices with axes perpendicular to the flow direction (a) Overall view (Photo: I.Wood, 1984) (b) Close-up of foam layer and vortex (Photo: N.Thomas in Goldring et al., 1980)

impinging on rigid walls (e.g. in self-priming configurations for siphons) produce a surface roller with self aeration resembling that of the hydraulic jump. Figure 1.6 shows flow configurations of the surface roller type, which are encountered most frequently in nearly horizontal flows.

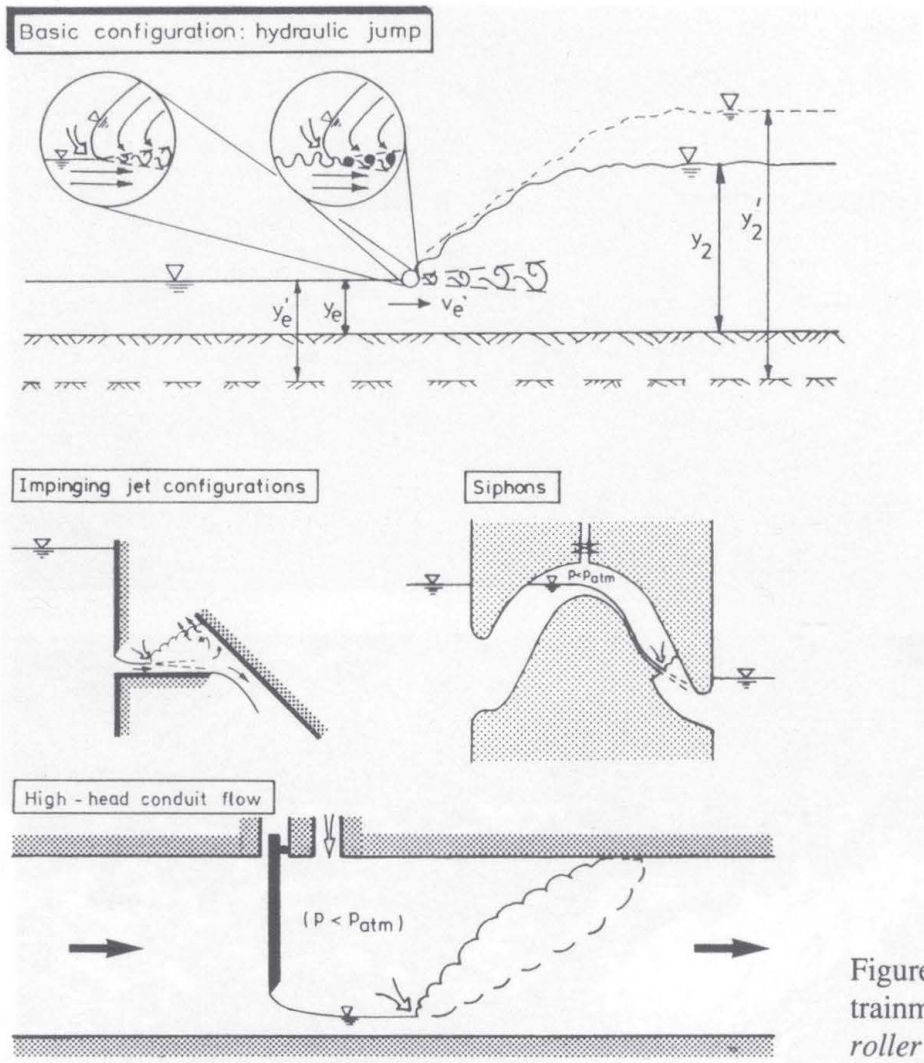

Figure 1.6. Local air entrainment at *surface-roller type* configurations

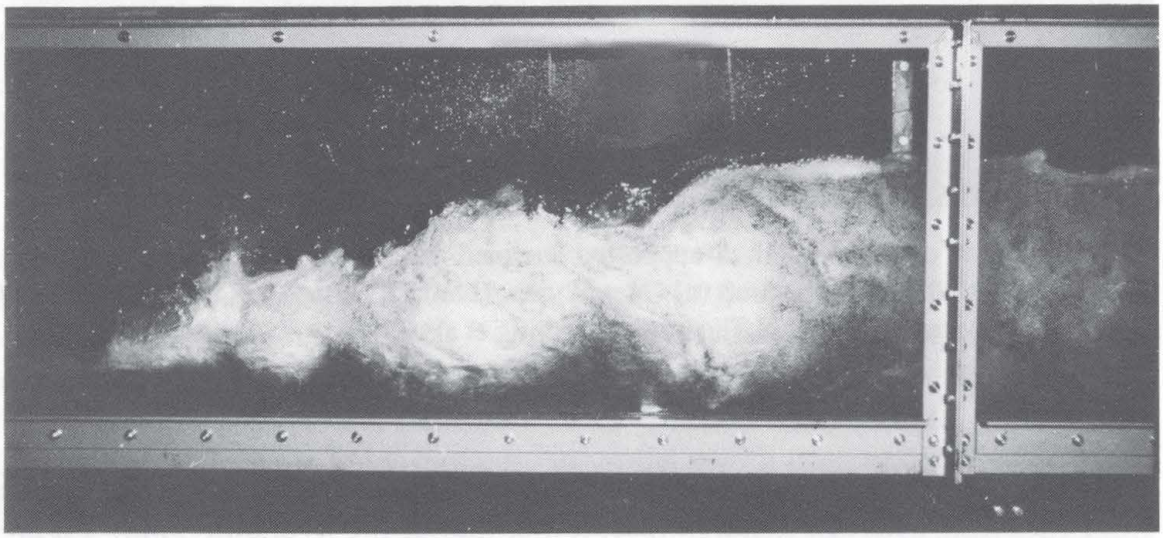

Figure 1.7. Air entrainment in a hydraulic jump caused by vortices with axes perpendicular to the flow direction (Photo: B. Barczewski, 1985)

1.2.4 *Local aeration in the wakes of bluff bodies*

Zones of flow separation in the wake of bluff bodies or at abrupt expansions of the cross section are characterized by a pressure significantly lower than that of the main flow. Bluff bodies protruding through the water surface therefore cause a marked surface depression in the separation zone. Also the boundary of flow separation penetrates the water surface. The intensive turbulence in the free-shear layer forms vortices (vortex axis perpendicular to flow) which may entrain air into their cores. Air entrainment is particularly pronounced near the channel side walls due to such effects at wall protrusions. Also, stilling basin blocks, piers or large rocks in fast flows exhibit this characteristic quite clearly.

The action of bottom offsets in spillways (as shown in Figures 1.8 and 1.9) or conduits can be approximately related to this type of air entrainment. However, the situation differs in three ways:

– the line of flow separation is horizontal and along the inclined bottom, rather than vertical and protruding through the water surface;

– the air supply is not directly from the atmosphere, but through an air duct system;

– air is entrained into the water upward from below, rather than downward from above as in all other configurations.

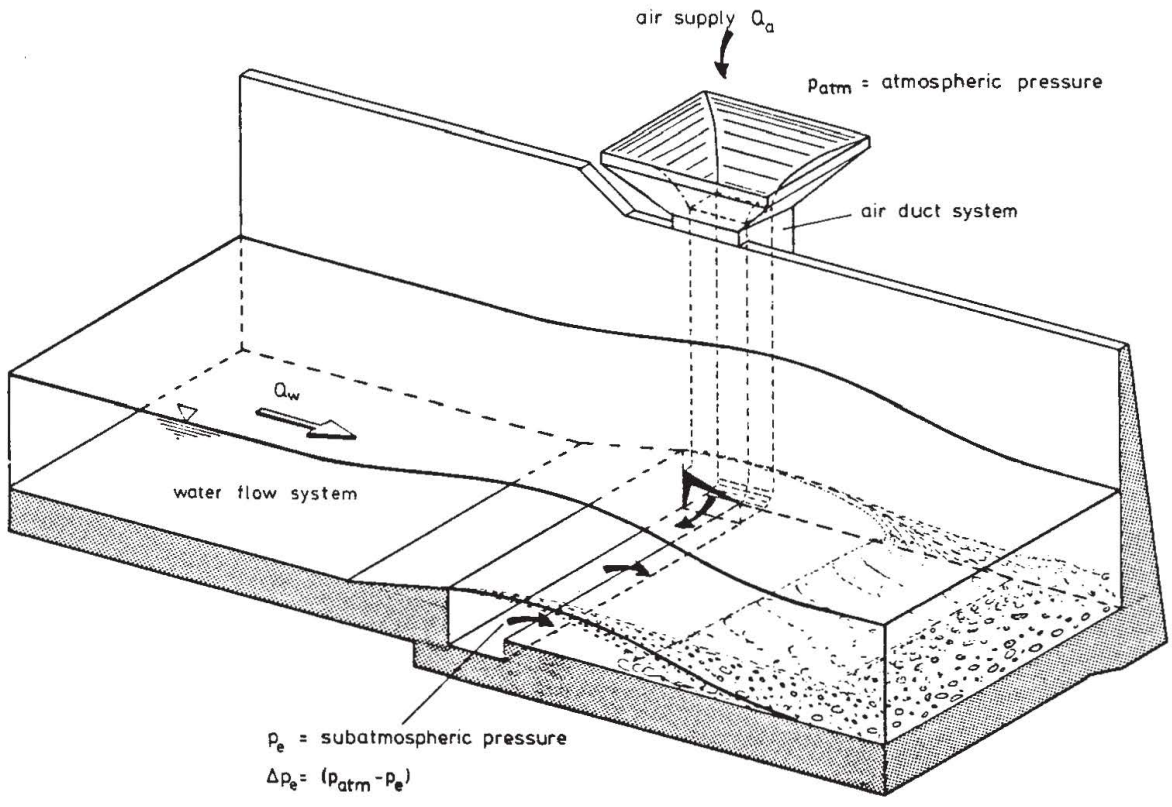

Figure 1.8. Air supply system of an aerator device

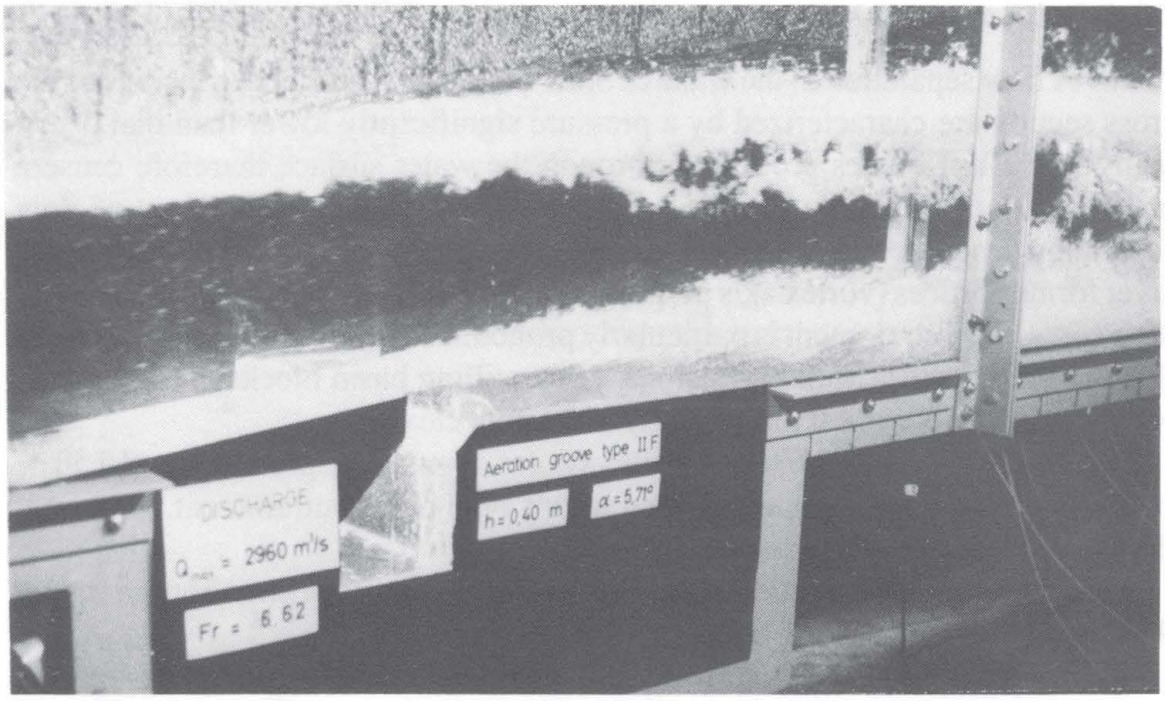

Figure 1.9. Air entrainment in an aerator device (Sectional model. Photo: H.-P. Koschitzky, 1984)

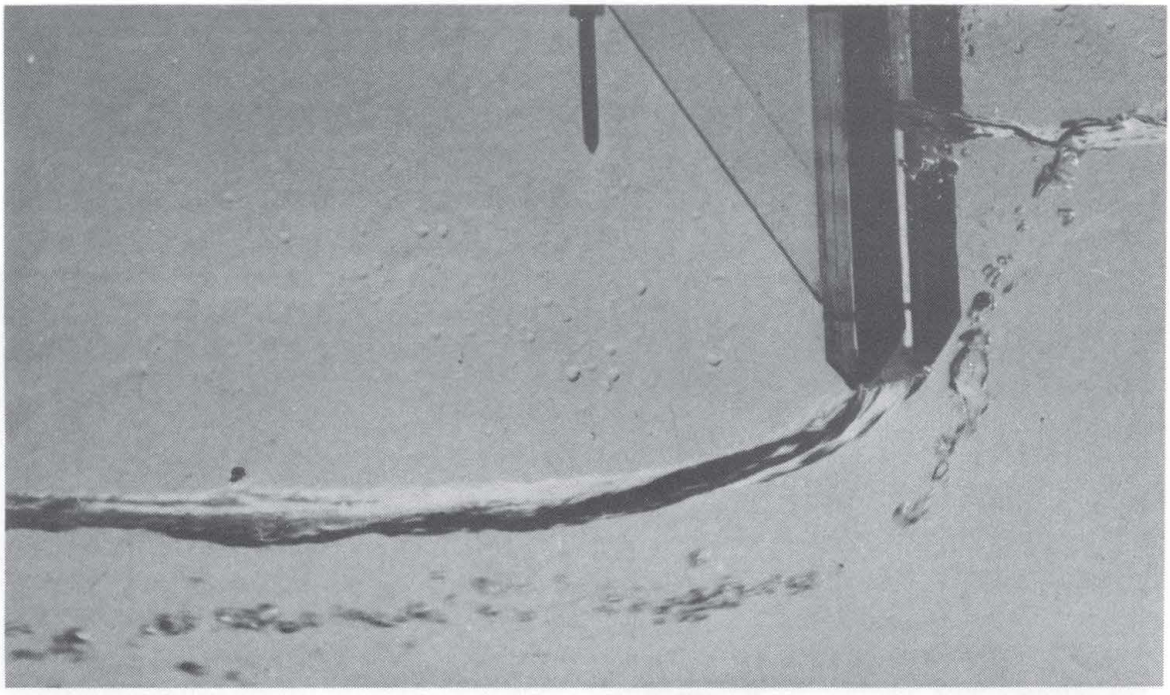

Figure 1.10. Air entrainment at a sluice gate by a vortex with an axis parallel to the flow. Similar flow conditions are encountered at intake structures. The vortex develops from the environmental vorticity in the approach flow (Photo: I. Wood, 1984)

1.2.5 *Local aeration at transitions from free-surface to conduit flow*

Transitions from free-surface to conduit flow are encountered at intake structures, pump sumps, control structures, gates, drop shaft spillways, etc. Upstream from the transition to pressurized flow, a region of stagnation occurs at the water surface, and depending upon the approach flow and boundary geometry, swirl and vortex formation may lead to air entrainment into the system.

In this case, air is entrained by distinct vortices with axes parallel to the flow direction. The major mechanism is the stretching of patches of environmental vorticity until the rotation of the core becomes sufficiently large and the consequent pressure sufficiently small for air to be drawn into the core. Figure 1.10 shows the flow under a sluice gate where the air at the core of such a vortex is apparent.

Air entrainment into closed-conduit systems is usually undesirable for such reasons as disturbances of pump performance or flow variations due to the detrainment and accumulation of air in the system. Further information on this distinctly different type of air entrainment is contained in the monographs: *Swirl-flow problems at intakes* and *Air-water flow in closed conduits*.

1.3 EFFECTS OF ENTRAINED AIR UPON THE WATER FLOW

Entrained air can strongly affect the performance of hydraulic structures for the following reasons:

– The bulk properties of the fluid (a mixture of air and water) are changed. This concerns mainly the density and the elasticity.

– The presence of air changes the structure of flow turbulence and possibly the wall shear as well.

– The presence of air helps to avoid excessive negative pressures and cavitation.

– Air bubbles introduce vertical momentum into the flow due to their buoyancy and may thus have significant effects upon the flow field.

– In open channels, entrained air leads to an increase in water depth (bulking).

– In spillway chutes, air near the bottom may lead to an increase in flow velocities.

– In closed conduits, for a given flow cross section the presence of air leads to changes in water discharge or pressure distribution in the system.

– The presence of air affects the performance of hydraulic machinery adversely.

– In hydraulic transients, pressure waves are strongly damped and deformed.

– Air accumulation in a system may lead to disruption of the flow and such effects as *blow-out* or *blow-back*.

– The presence of air bubbles leads to intensive oxygen and nitrogen transfer until the surrounding water has reached saturation.

Air entrainment is in some cases desirable and in others undesirable. It is desirable, e.g. for cavitation prevention, for oxygenation and for the damping of hydraulic transients; undesirable examples include effects on pumps, on intake structures and in closed conduit systems.

1.4 THE ROLE OF THE TRANSPORT CAPACITY

A self-aerating flow configuration continuously produces air bubbles by mechanical action, which are subsequently carried away by the flow if the transport capacity of the water flow is sufficiently high. All those bubbles which are entrained but cannot be transported by the flow will escape through the water surface (detrainment). Thus air entrainment, transport capacity and detrainment are interrelated. For a given configuration, the air entrainment is governed by the upstream conditions, whereas the transport capacity depends entirely upon the downstream water flow configuration. If the transport capacity is zero (as in stagnant or slowly flowing water bodies), then all entrained air will detrain.

The transport capacity of the water depends primarily upon the ratio between water velocity v_w and bubble rise velocity v_b. In stagnant water bodies ($v_w << v_b$), the transport capacity is zero. The air bubbles will rise to the surface due to their buoyancy and escape. In slowly flowing water ($v_w \approx v_b$), the entrained air bubbles are displaced by the water flow and the flow field may be changed drastically by the air bubbles.

In high-speed flows in open channels ($v_w >> v_b$), the transport capacity increases with increasing velocity (i.e. channel slope) and turbulence intensity of the water flow. The transport capacity is characterized by an equilibrium between the rising tendency of the bubbles and the counteracting mixing effect of the turbulent fluctuations in a concentration gradient, quite analogous to the transport of suspended solids (although bubbles do show several distinct differences to solid particles).

In closed conduit flow, the transport capacity is additionally dependent upon the orientation of the flow with respect to the direction of the buoyancy force. Obviously, the transport capacity will be a maximum in vertically upward flow and a minimum for vertically downward flow.

Whenever the local air entrainment exceeds the transport capacity of the subsequent channel or conduit, detrainment will take place. The resulting net detrainment can be expected to be proportional to the amount of air in excess of the transport capacity. A hydraulic jump, for instance, entrains a considerable amount of air locally, but because of little or no capacity for air transport most of it escapes back into the atmosphere through the surface roller, so that only a short distance downstream the air content of the flow is almost zero again.

If the transport capacity is exceeded in conduit flows, the *detraining air* will collect at the top of the conduit and form air pockets. Depending upon the flow velocity and the inclination of the conduit, these pockets will grow and after they have reached a certain size, may move in the direction of flow or against it. The resulting unsteady flow conditions can cause sizable pressure fluctuations and flow instabilities in the system (*blow-out* or *blow-back*).

1.5 PARAMETERS FOR AIR-WATER FLOWS IN OPEN CHANNELS

For open channel flows as discussed in this monograph, there exist

- always unlimited air escape directly to the atmosphere;
- usually unlimited air supply directly from the atmosphere (with the exception of spillway aerators or weir aeration);
- a direct dependence of the transport capacity upon the characteristics of the open channel flow.

These conditions exclude a priori any effects of independent variation of flow inclination or of limited air escape with feedback upon the flow, as may be encountered in pressurized flow in closed conduits. These latter aspects will be treated in the monograph *Air-water flow in closed conduits*.

The dependent variables describing the air entrainment, transport and detrainment process are air flow rates Q_a or q_a, resulting bubble sizes d_b, air concentrations c_a and bulk dimensions of the air-water mixture, as well as trajectories and residence times of bubbles. In air flow rates, we have to distinguish

- the total rate of entrained air, Q_{ae}
- the specific rate of entrained air q_{ae} (per unit width)

and in contrast to these

- the total air transport rate Q_{at}
- the specific air transport rate q_{at}.

All of the dependent variables can be described in terms of independent variables representing

- boundary geometry: reference length l_w; geometric lengths;
- water approach flow: reference velocity v_w; (turbulence Tu);
- air supply system: pressure difference Δp_e;
- fluid properties: ρ_w; g; μ_w; σ_{wa}.

The fluid properties of air can usually be neglected. For a given geometry, this set of variables also characterizes the downstream flow conditions.

For the dependence of the specific rate of entrained air, for instance, we can now write

$$q_{ae} = f(\text{geometry}; l_w; v_w; (Tu); \Delta p_e; \rho_w; g; \mu_w; \sigma_{wa}) \tag{1.1}$$

where the left hand side could be any other dependent variable of interest. A classical dimensional analysis leads to

$$\frac{q_{ae}}{v_w l_w} = f(\text{geom. ratios}; (Tu); \frac{\Delta p_e}{\rho_w v_w^2/2}; \frac{v_w}{\sqrt{g l_w}}; \frac{v_w l_w}{\mu_w/\rho_w}; \frac{v_w}{\sqrt{\sigma_{wa}/\rho_w l_w}}) \tag{1.2}$$

or

$$\beta_e = q_{ae}/q_w = f(\text{geom.ratios}; (Tu); c_{pe}; Fr; Re; We) \tag{1.3}$$

and alternatively, replacing *We* by the rules of dimensional analysis by the parameter *Z* (Kobus, 1973) to

$$\beta_e = f(\text{geom.ratios}; (Tu); c_{pe}; Fr; Re; Z \equiv (g\,\mu_w^4)/(\rho_w \sigma_{wa}^3) \tag{1.4}$$

and corresponding relationships for all other dependent variables, including the turbulent flow characteristics like turbulence intensity or turbulent energy spectrum. The relationship (Equation 1.4) represents the general similarity requirements for local aeration processes.

As an alternative to the Weber number, which describes the relative importance of inertial forces and surface tension, the liquid parameter *Z* can be used. This parameter has the obvious advantage that it contains neither the reference length nor the reference velocity. It is a function of the liquid properties alone and thus independent of the boundary scale and the flow velocity. For pure water, the value of the liquid parameter is ($Z \approx 10^{-11}$); it will remain constant as long as temperature and water quality remain unchanged. In evaluating small scale model studies, this set of parameters has the advantage that *scale effects* in Froude models, for an invariant *Z*, are now concentrated in the effects of the Reynolds number. Otherwise, Equations 1.3 and 1.4 are completely equivalent.

1.6 GENERAL CONTROLLING CONDITIONS

The process of air entrainment is subject to several limiting conditions: an inception limit, entrainment limit, air supply limit and transport limit. Each one of these may be the controlling factor: therefore, in comparing flow configurations of different geometry or size, attention has to be paid to all of these limits.

Inception limit

For a give flow configuration, the flow conditions must be such as to generate a sufficiently large disturbance for air entrainment to occur. The inception limit depends strongly upon the fluid properties and characterizes the condition that inertial reactions become large enough to overcome the resisting forces due to viscosity and surface tension. In general, a certain minimum velocity has to be exceeded, and the initiation of air entrainment is greatly enhanced by turbulent fluctuations of the approach flow.

Entrainment limit

The conditions of the approach flow govern the entrainment limit. These conditions are quantified by the Froude number *Fr*. Depending upon the boundary geometry, a critical value of *Fr* must be exceeded to ensure the formation of a surface disturbance or discontinuity at which air entrainment can occur (e.g. $Fr > 1$ for the hydraulic jump). For higher Froude numbers, the approach flow provides the driving mechanism for the air entrainment. In most cases, the air entrainment process is not directly affected by the local boundary scale.

Air supply limit

In flow configurations such as spillway aerators (Figures 1.8 and 1.9), ventilation ducts in dropshaft systems or air shafts in closed conduits, air is entrained from a limited enclosed air space, which is connected to the atmosphere by an air duct. In these cases, the supply of air to the point of entrainment into the water requires an air flow through a duct system. This flow necessarily results in a pressure difference between the ends of the air duct. The subatmospheric pressure at the location of air entrainment depends upon the air entrainment rate and the air duct resistance. As shown in Figure 1.11, the pressure difference is a maximum if the air duct is closed and decreases to zero for unlimited air supply. The head loss characteristics of the air duct system determine an operating point characterizing the resulting air supply rate and the corresponding pressure difference. In this case, the air supply system is limiting the air entrainment.

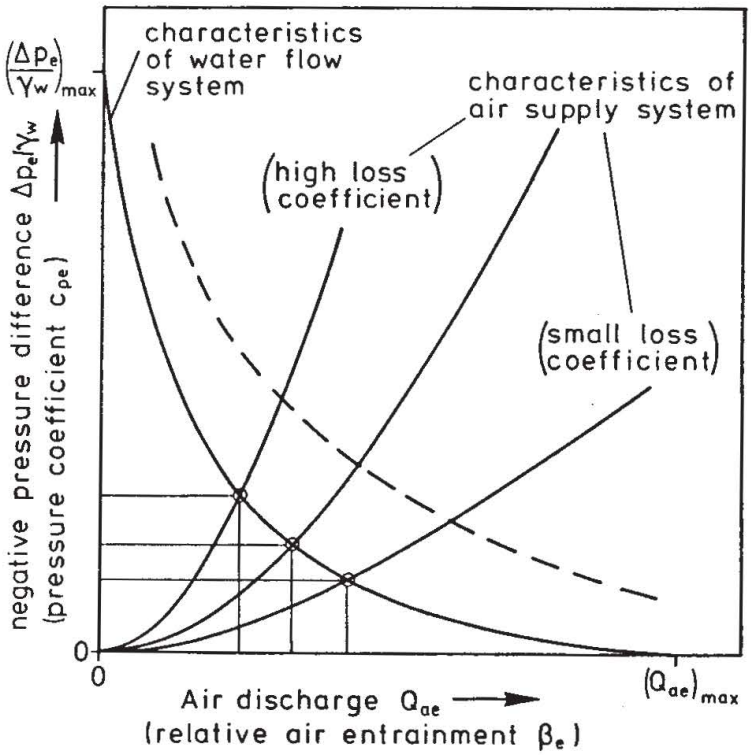

Figure 1.11. Air supply control

Transport limited
The transport capacity of the flow is governed by the downstream flow conditions. It depends upon the flow velocity and turbulence as determined by the wall shear stresses (Wood, 1983). An upper limit for air transport is given by the maximum possible air bubble concentration in the flow (Brauer, 1971).

1.7 AIR BUBBLE FORMATION AND TRANSPORT

1.7.1 *Bubble formation*

The process of air entrainment involves the entrapment of an air volume at the surface, the breakup of the entrapped air volume into an array of bubbles, and the subsequent transport by the flow, during which the bubble size distribution may change due to coalescence or breakup of individual bubbles. At the entrainment location, air is entrapped in the low pressure cores of vortices and is transported into the water until the cores decay and the pressure differences become small, and the air bubbles are released. Whereas the entrapment and initial breakup are governed by inertial and gravitational forces and are hence Froude-number dependent, the bubble transport is governed by viscosity through the turbulence characteristics and hence relate to the Reynolds number of the flow.

The entrapment and bubble formation process at local surface discontinuities is related to the turbulent shear stress generated between approach flow and receiving water body. Here, the scale and intensity of the turbulent fluctuations in the approach flow play a predominant role. Ervine (1985), argues that the bubble diameter generated is a function of the turbulence characteristics at the entrainment location, with peak turbulence levels entraining small air pockets, median turbulence levels entraining mean size air pockets, etc. He therefore concludes from the fact that the shear layer turbulence shows a Gaussian distribution that the resulting bubble diameters should also follow a Gaussian distribution curve.

A frequently investigated process of bubble formation is the breakup of a continuous air jet discharging from a nozzle into a water body. Analytical considerations on instability and breakup of air pockets by Rayleigh have been verified experimentally (Kobus, 1973). If air is injected continuously through a nozzle into an otherwise stagnant water body, the air jet immediately breaks up into an array of bubbles which range in a diameter from almost zero up to a maximum value, which depends upon the air discharge Q_a and gravitational acceleration g (Kobus, 1973):

$$d_{b,\max} = (1.295 \text{ to } 1.487)\,(Q_a^2/g)^{1/5} \qquad (1.5)$$

In free-surface aeration, the mixture of bubbles will also occur up to a certain

maximum size; no information is available, however, about the magnitudes involved.

Numerous visual observations and some measurements of bubble sizes in turbulent flows (excluding here high speed flows with $v_w >> v_b$) have shown that the majority of the large bubbles are in the range of 1 to 10 mm, and that the mean bubble diameter decreases with increasing turbulence. Some examples of measured bubble size distributions in air bubble screens are shown in Figure 1.12. These observations suggest that turbulent flows of air-water mixtures should finally reach a state of equilibrium with a certain turbulence structure corresponding to a distribution of bubble sizes.

In high-speed flows ($v_w >> v_b$), the range of resulting bubble sizes is probably smaller than that given above. The higher the resulting shear rates, the smaller will be the air bubbles. Observations of flow on spillways indicate that bubble sizes are small near the bed and increase with increasing distance from the bed.

Air bubbles of finite size always exhibit a slip velocity v_b relative to the surrounding water. To an acceptable degree of approximation, this slip velocity corresponds to the rising velocity of a single bubble in an infinite fluid or otherwise at rest. The flow field can therefore be considered as a combination of the water flow field with the bubble slip velocity superimposed (In high-speed flows, this effect is small).

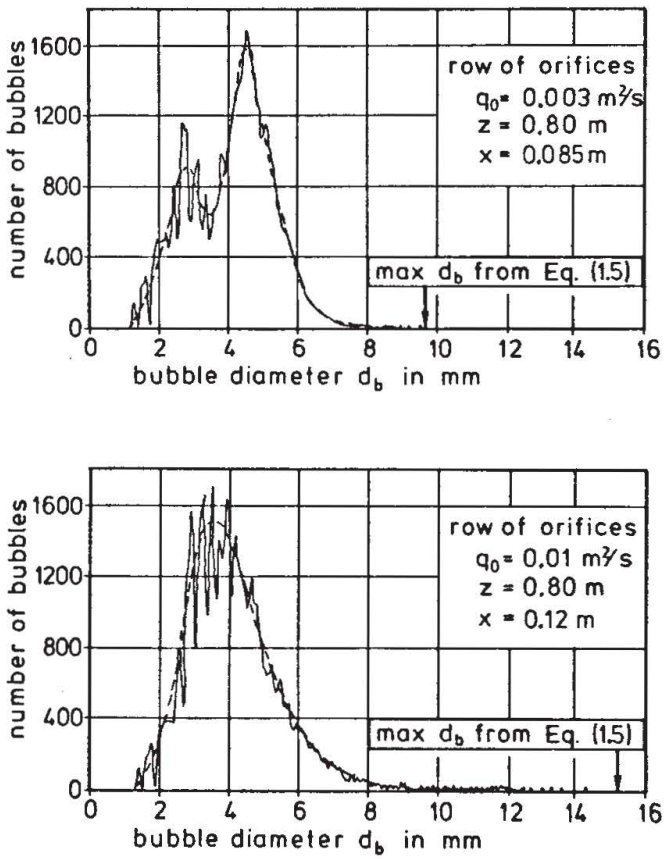

Figure 1.12. Examples of bubble size distributions in turbulent flow: Measurements of Barczewski (1979) in a plane bubble plume at an elevation z and lateral distance x from plume axis

1.7.2 *Bubble slip velocity: single bubble in stagnant water*

The behaviour of a single gas bubble in a liquid has been studied extensively. A dimensional analysis for the bubble rise velocity v_b of a bubble of diameter d_b yields

$$c_d \equiv \frac{4g.d_b}{3v_b^2} = f\left(Re \equiv \frac{v_b d_b}{\mu_w/\rho_w}; Z \equiv \frac{g.\mu_w^4}{\rho_w \sigma_{wa}^3}\right) \tag{1.6}$$

The definitions are given in the list of symbols.

The quantitative relation between these parameters is given in Figure 1.13. This diagram shows a nearly universal relation between c_d and Re, in which the influence of the liquid parameter Z is pronounced only in the region of Reynolds numbers between 10^2 and 10^3. Thus, for Reynolds numbers smaller than 10^2 (small bubbles) and larger than 10^3 (large bubbles) the c_d-versus-Re relation can be considered as universal and valid for any kind of gas or liquid, whereas in the intermediate region ($10^2 < Re < 10^3$), the liquid parameter Z (and hence the water quality) plays an important role.

For the case of very small spherical bubbles, an exact expression has been obtained for the relationship. Surface tension is the predominant force determining the shape of very small bubbles. Therefore, small bubbles tend to be almost perfect spheres. The motion of these bubbles through a fluid can be described by a balance between the buoyant forces and the viscous forces. Since the bubble behaves like a rigid sphere, Stokes solution applies:

$$c_d = 24/Re \qquad \text{for small } Re \tag{1.7}$$

The region of validity of this relation depends upon the magnitude of Z (see Figure 1.13). In terms of the bubble rise velocity v_b, this can be expressed as

$$v_b = \frac{1}{18}\frac{d_b^2 g}{\upsilon_w}\left(1 - \frac{\rho_a}{\rho_w}\right) \qquad \text{for small } Re \tag{1.8}$$

For slightly larger bubbles, a spherical shape and straight rising path is maintained, but an internal gas circulation is set up which results in a relationship of the form

$$c_d = 16/Re \qquad (\text{for } Re < 10^2) \tag{1.9}$$

or in terms of bubble rise velocity

$$v_b = \frac{1}{12}\frac{d_b^2 g}{\upsilon_w}\left(1 - \frac{\rho_a}{\rho_w}\right) \qquad (\text{for } Re < 10^2) \tag{1.10}$$

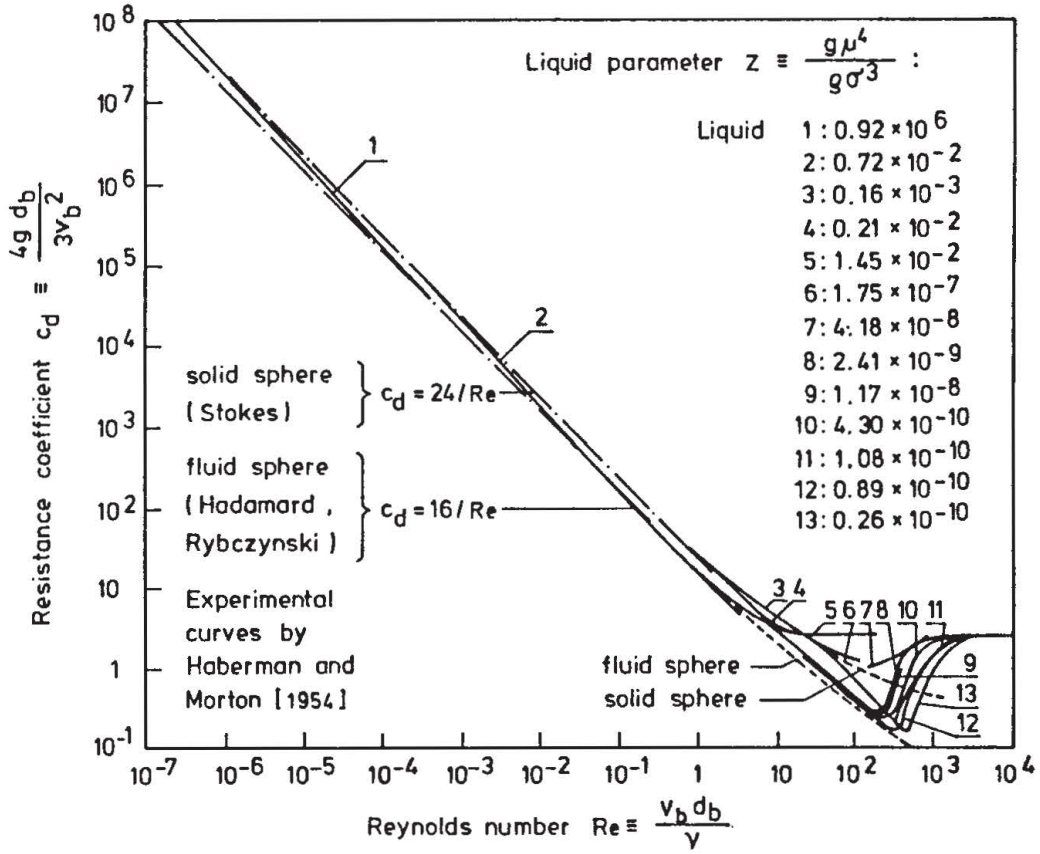

Figure 1.13. General resistance diagram for gas bubbles in liquids

The transition to this range depends strongly upon the liquid parameter Z. For water, which has an extremely low value of ($Z \approx 10^{-11}$), no experimental evidence for this flow regime is known.

As the bubble becomes larger, inertial effects become important and the bubble shape changes in accordance with the pressure distribution over the surface. With increasing size, the bubble shape changes to an oblate spheroid, and the bubble rises along an irregular or spiral trajectory. For this region, numerous empirical formulae describing the bubble rise velocity have been proposed. However, all of these relations are valid only for a limited range and are strongly influenced by the liquid parameter Z.

Very large bubbles attain a spherical cap shape with an included angle of the spherical front surface of about 100 degrees and a relatively unstable flat base. These large bubbles follow again a straight rising path. The bubble rising velocity in this range is characterized, according to Haberman & Morton (1953), by

$$c_d = 2.6 = \text{const} \qquad \text{for } (Re > 2 \,.\, 10^3) \qquad (1.11)$$

or else

$$v_b = 0.716\, g\, .\, d_b \qquad \text{for } (Re > 2\, .\, 10^3) \qquad (1.12)$$

For the specific case of air bubbles in natural water bodies, the relationship between terminal rising velocity and equivalent bubble diameter (diameter of sphere of equal volume) is shown in Figure 1.14. This relationship has been determined experimentally by Haberman & Morton (1953). It exhibits the same parameter dependence as Figure 1.13. For the fluid properties of air and water at 10°C of

$$\upsilon_w \approx 1.3 \times 10^{-6}\ \mathrm{m^2/s}$$
$$\rho_w \approx 1000\ \mathrm{kg/m^3}$$
$$\rho_a \approx 1.25\ \mathrm{kg/m^3}$$

one obtains the following dimensional relationship for small bubbles, corresponding to Equation 1.8 for ($Re < 1$):

$$v_b\,|\mathrm{m/s}| = 0.362\, d_b^2\,|\mathrm{mm}| \qquad \text{for } (d_b < 0.2\ \mathrm{mm}) \qquad (1.13)$$

For intermediate bubble diameters between 0.2 and 20 mm, the air bubble rising velocity can be taken from Figure 1.14. In this range, variations due to water quality (i.e. variations of the parameter Z) are evident, with velocities anywhere between 0.1 and 0.4 m/s. Ellipsoidal shapes and spiral motions occur for bubble diameters exceeding 1 to 2 mm. In pure water, a pronounced maximum velocity is observed for bubbles slightly larger than 1 mm in diameter. In contrast, contami-

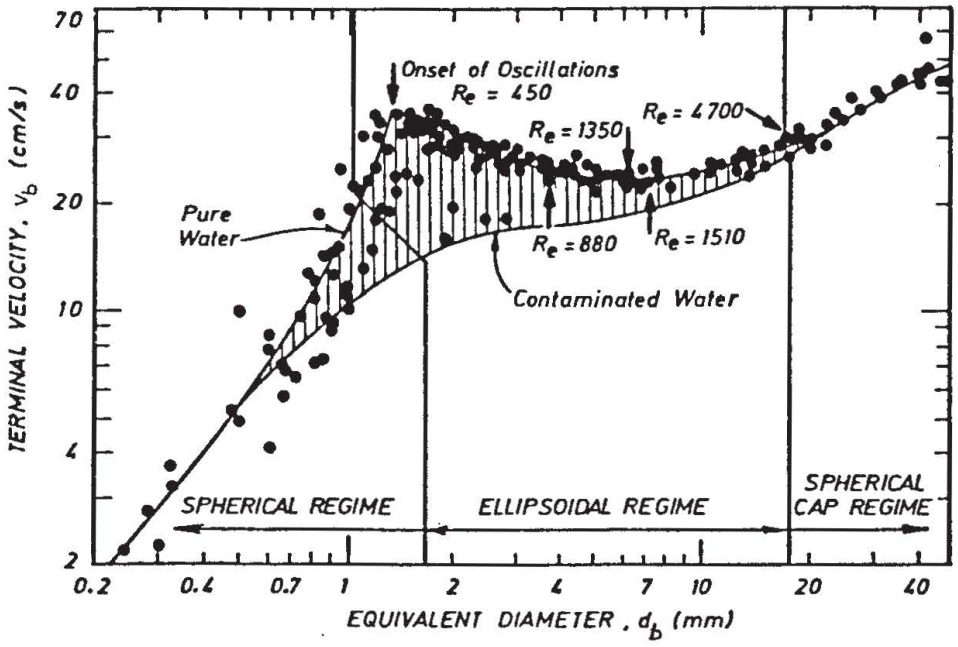

Figure 1.14. Terminal bubble rise velocity v_b of a single air bubble in an extended body of water otherwise at rest (Haberman & Morton, 1954)

nated water does not exhibit this peak and gives considerably different values.

For very large bubbles of spherical cap shape, one obtains a unique relationship corresponding to Equation 1.12 as

$$v_b|\text{m/s}| = 0.071\, d_b^{1/2}|\text{mm}| \qquad \text{for } (d_b > 20\text{ mm}) \qquad (1.14)$$

1.7.3 *Motion of a bubble cloud in stagnant and moving water*

If a multitude of air bubbles is released in a laterally unrestricted stagnant water body, the ensemble will rise to the surface with a considerably larger mean velocity than a single bubble. This results from the fact that the bubble swarm induces an upward water flow (due to the preceding and surrounding bubbles) which adds to the individual bubble slip velocity. On the other hand, if the water has a horizontal velocity component, this effect is counteracted to some degree by the fact that the bubbles are displaced laterally along their path and hence the induced vertical water flow is less pronounced. An air bubble plume is shown in Figure 1.15.

Figure 1.15. Air bubble plume

As an indication of the magnitude of the effects involved, Figures 1.16 and 1.17 show some experimental data for average rising speeds of bubble clouds above single orifices and above rows of orifices, respectively. These data demonstrate two points:

1. The air bubbles induce a substantial vertical water velocity, leading to effective rising velocities which are two to three times higher than those for a single bubble.
2. Even moderate cross flow velocities dramatically counteract this bubble-induced flow and quickly reduce bubble-rise velocities again to the order of magnitude of the slip velocity of single bubble.

The air bubble plumes described above rise in a laterally unconfined flow. In the presence of lateral confining boundaries, the mean rising velocity will be hindered by the fact that the displaced water will induce a downward counterflow for continuity reasons – much in the same way as the side wall effect of a narrow tube affects the settling of a single particle. In flow configurations where bubbles occur in the entire flow region (as on spillways, e.g.), the mean bubble rising velocity must by continuity be the hindered velocity.

1.7.4 *Effects of pressure gradient upon air-bubble motion*

The motion of air bubbles is usually considered in water bodies with a more or less hydrostatic pressure distribution. In this case, the bubbles rise vertically upwards. If the pressure distribution is changed, the air-bubble motion may be greatly affected. For instance, in a freely falling jet with no pressure gradient, the resulting force on the bubble and hence its slip velocity vanishes. An extreme situation is encountered in spillway aerators (Figures 1.8, 1.9). Because of the subatmospheric pressure below the nappe, a pressure gradient across the water flow results which is opposite in sign to the hydrostatic case. Therefore, the bubbles experience a downard force and hence move downward relative to the surrounding water.

1.7.5 *Effect of turbulence upon air bubbles*

Air bubbles are greatly affected by flow turbulence. This is primarily turbulence in the carrying water flow generated either by wall shear (bottom friction) or by free shear layers (jet impingement, surface roller, separation zones). However, the presence of the air bubbles also contributes to the turbulent fluctuations (bubble-induced turbulence), and in stagnant water this is the only source of turbulence.

Turbulent fluctuations can be responsible for

- breakup of large air bubbles due to shear action;
- coalescence of small bubbles in the core of vortices in the flow, since the air follows pressure gradients in the flow much more rapidly than water because of its much smaller inertia.

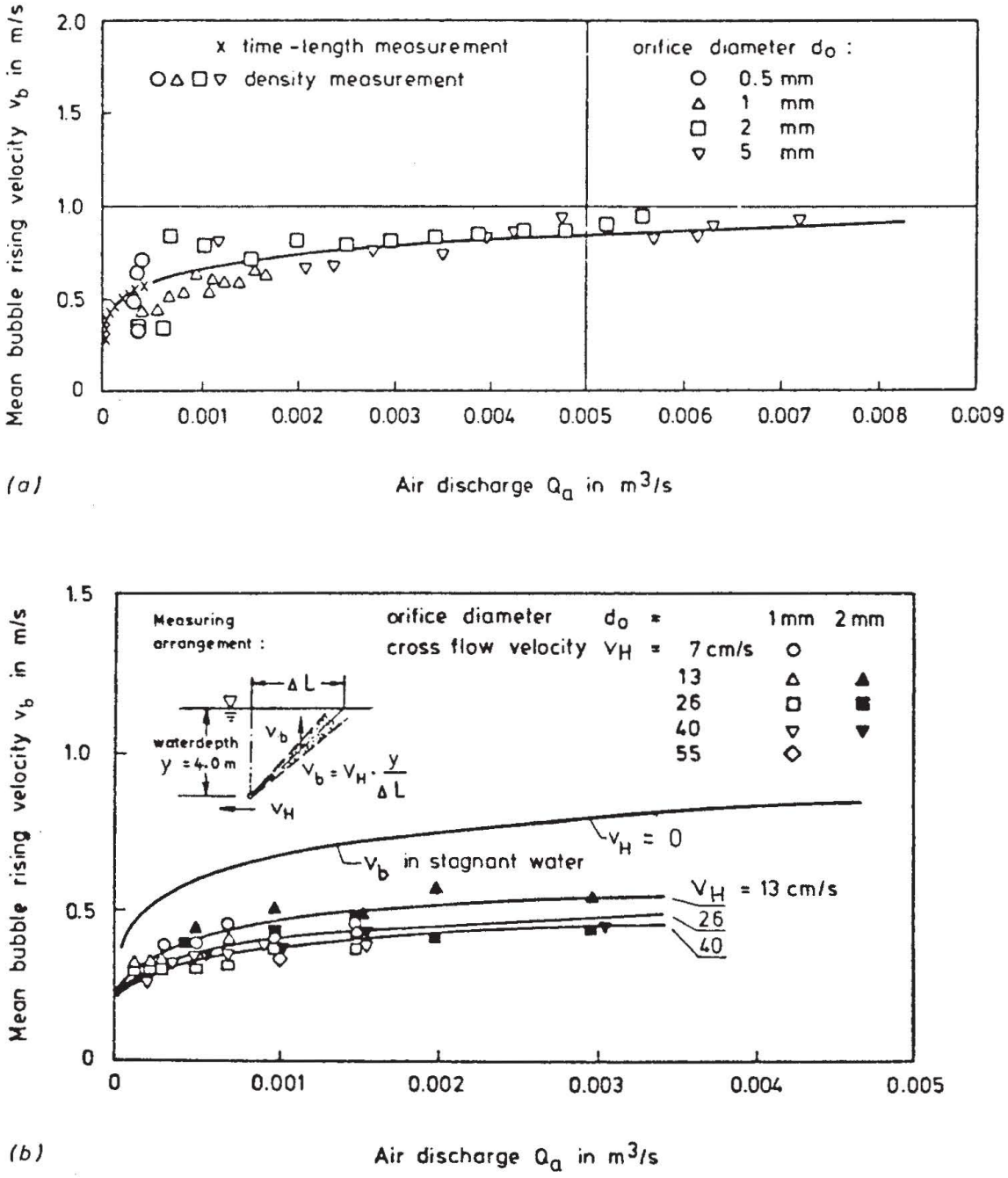

Figure 1.16. Mean rising velocity of bubble ensembles in a bubble plume above a single orifice (a) In stagnant water (b) In a cross flow

In open channel flows, the water flow is primarily in a direction parallel to the channel bottom, and the wall-friction-induced turbulent fluctuations (RMS) $v_t = \sqrt{\overline{v'^2}}$ increase to a first approximation linearly with the main water flow velocity v_w. By comparing the water flow velocity v_w to the bubble velocity v_b, which is of the order of magnitude of 30 cm/s, one can hence distinguish:

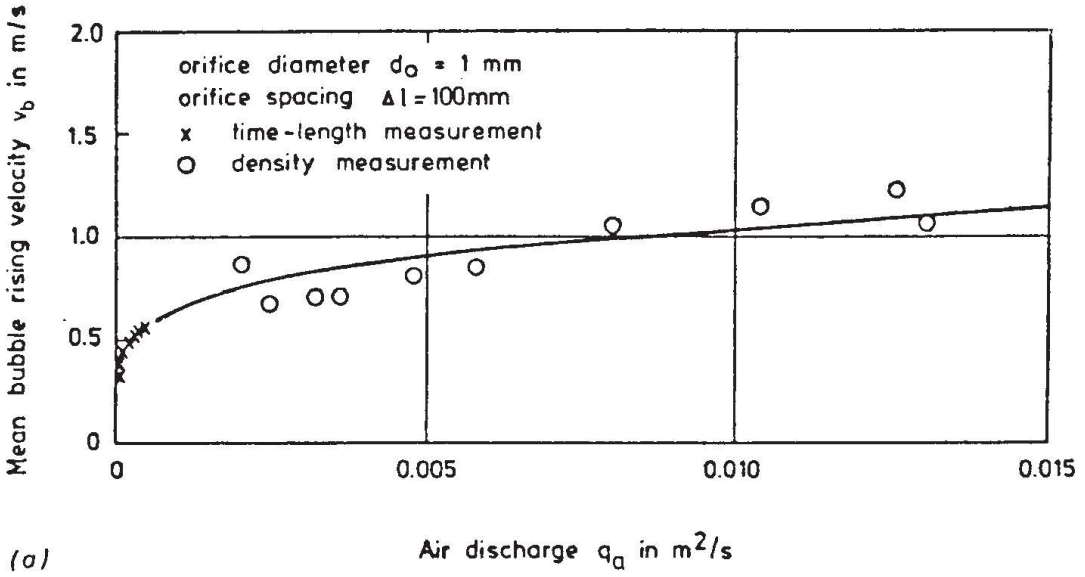

(a)

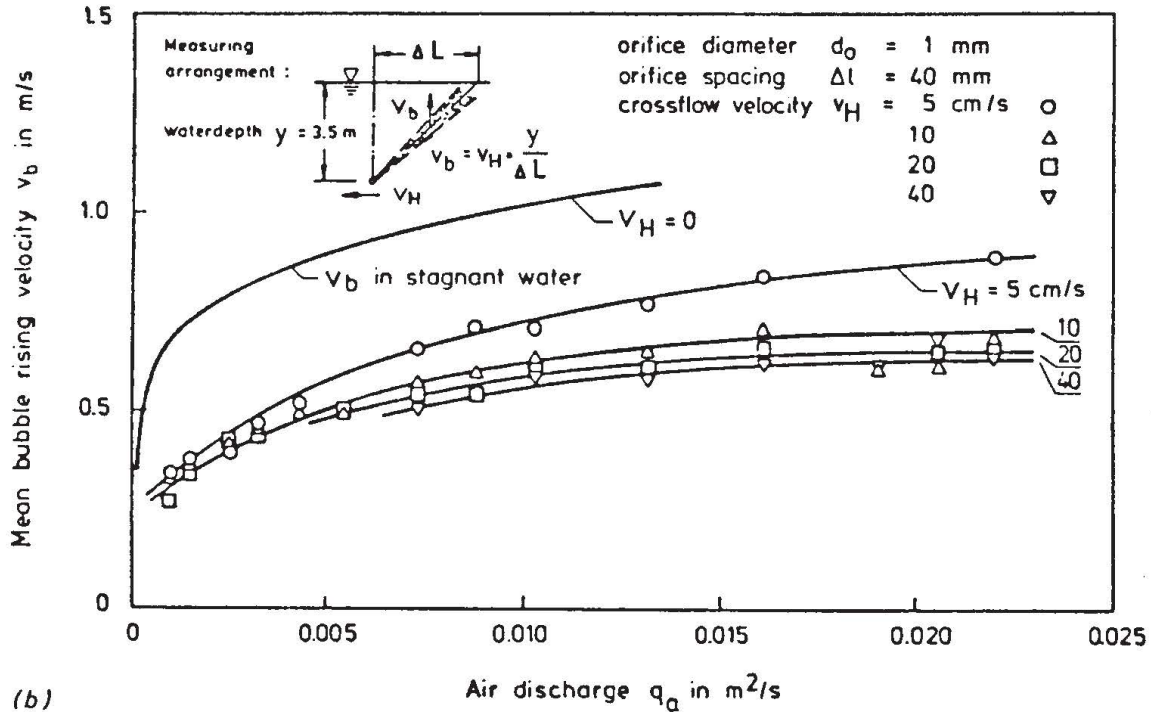

(b)

Figure 1.17. Mean rising velocity of bubble ensembles in a plane bubble plume (row of orifices) (a) In stagnant water (b) In a cross flow

– Nearly stagnant water bodies ($v_w \ll v_b$) such as lakes or reservoirs, with essentially bubble-induced turbulence,

– slowly flowing water ($v_w \approx v_b$) with pronounced air-water interaction, and

– high-speed flows ($v_w \gg v_b$) with pronounced effects of the water flow turbulence upon the air bubbles. For this range, Thomas et al. (1983) studied the

entrapment and transport of small bubbles by discrete vortices in a shear layer. Using both a numerical and a physical model, they showed that small air bubbles rising in water are trapped and transported by the vortices.

1.8 BUBBLE-INDUCED WATER FLOW

In stagnant water ($v_w << v_b$) or in slowly moving water ($v_w \approx v_b$), the effects of the bubbles on the flow field may be quite pronounced. The entrained air bubbles exert a buoyancy force on the surrounding water, which gives rise to a bubble-induced water flow. This process can best be illustrated for a bubble plume generated by injection of compressed air at the bottom of an otherwise stagnant water body. The resulting mean flow field and the turbulence is entirely due to the buoyany of the air and to the dynamics of the bubble swarm (purely bubble-induced turbulence).

The flow field of air and water in bubble plumes (Kobus, 1973) is characterized by the fact that the vertical momentum flux of the induced water flow increases with upward distances from the air source due to the continued action of the bubble buoyancy. The buoyancy force input F_B per unit time is given by the amount of entrained air:

$$F_B = (\rho_w - \rho_a)\, g \cdot Q_a = \rho_w g\, Q_a \tag{1.15}$$

and with this the vertical moment flux $M_{w,z}$ can be expressed as

$$\frac{dM_{w,z}}{dz} = F_B - F(v_b) \tag{1.16}$$

with $F(v_b)$ representing the resistance force to the slip velocity v_b. If the bubbles would be infinitely small (i.e. zero slip velocity and hence also $F(v_b) = 0$), then the flow field should correspond to the classical buoyant plume. However, bubbles of finite size do exhibit a slip velocity v_b relative to the surrounding water, which results in a correspondingly smaller increase of the water momentum flux. Part of the buoyancy force F_B moves the air bubbles through the liquid against the resistance force $F(v_b)$ to the slip velocity, and the remaining part acts to increase the water momentum flux $M_{w,z}$.

This fact illustrates the importance of the bubble sizes in determining the concentration and velocity distribution: the larger the bubbles, the higher the slip velocity v_b and the less pronounced the induced water velocity.

In contrast, the horizontal momentum flux of the water flow remains essentially unaffected by the presence of the air bubbles. The negligible density of the air bubbles allows them to be transported laterally by the water flow without significant slip. The only noticeable change for the horizontal flow components

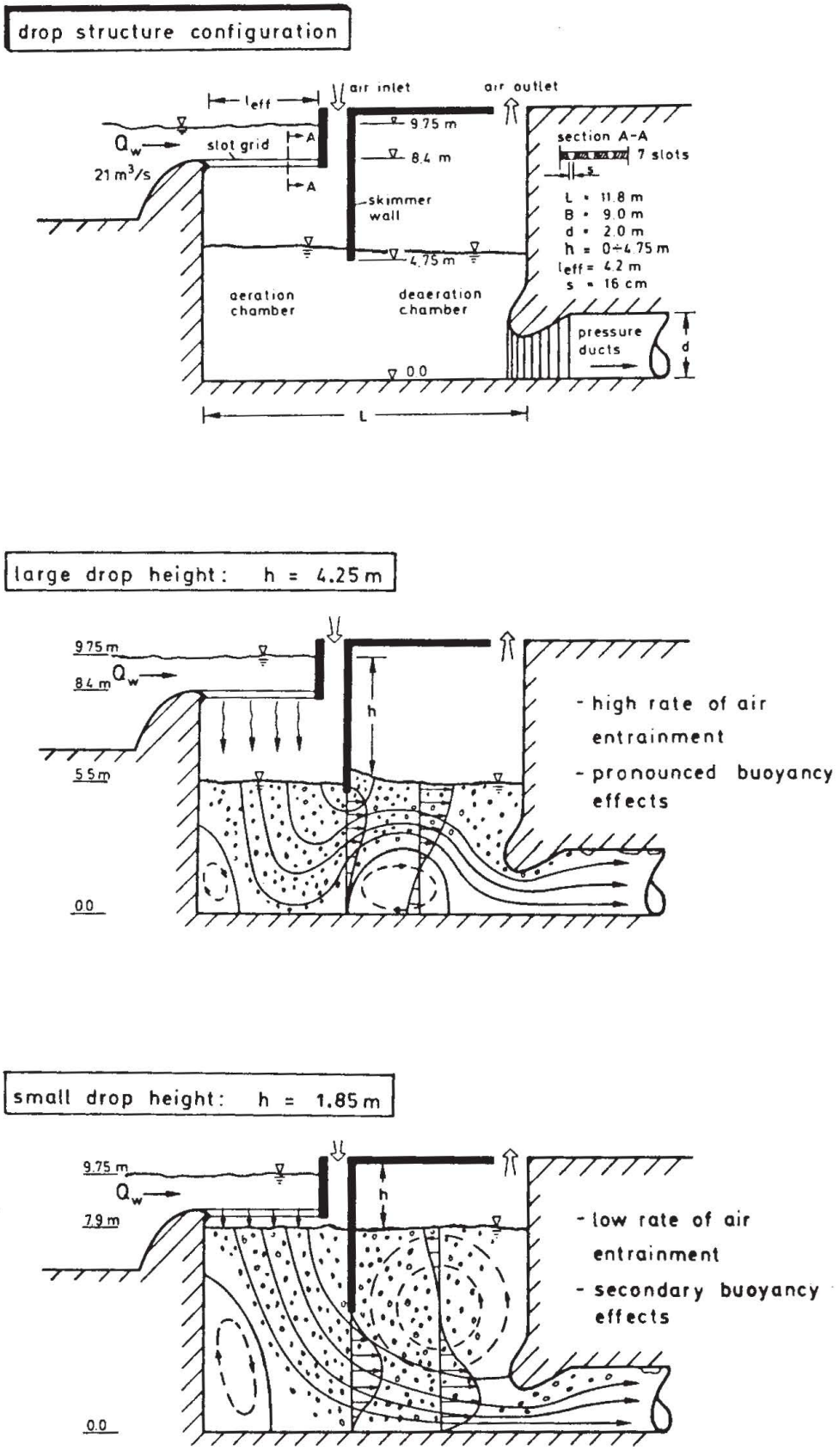

Figure 1.18. Effects of air buoyancy on the flow field in a drop structure (Kobus & Westrich, 1983)

due to high air concentrations will therefore be its effect upon the local mixture density. It follows that the most pronounced effects of air bubbles upon the water flow occur in predominantly vertical flow configurations, such as plunging jets or in drop shafts, and that, they play a lesser role in predominantly horizontal flows.

As an illustrative example for the drastic effects that entrained air can have on the water flow field, two flow situations in a drop structure are shown in Figure 1.18, which are described in detail by Kobus & Westrich (1983). A comparison of the flow configuration with a high rate of air entrainment (middle part) with the flow field at a low rate of air entrainment (lower part) shows that the presence of the strong bubble entrainment and detrainment affects the water flow to the extent that the location of flow separation is changed and that the direction of flow rotation in the separation zone is reversed.

In high-speed flows (e.g. on spillways) with water velocities much larger than the bubble rising velocities, the dynamic effects of the air bubbles on the flow are negligible and the bubbles behave almost like inert tracers or like fine suspended sediment particles.

LIST OF SYMBOLS

c_a	[%]	air concentration
c_d	[–]	drag coefficient (resistance coefficient)
c_{pe}	[–]	pressure coefficient $c_{pe} = \Delta p_e/(\rho_w v_w^2/2)$
D,d	[m]	diameter
d_b	[m]	equivalent bubble diameter (sphere of equal volume)
d_o	[m]	orifice diameter
F_B	[N]	buoyancy force
$F(v_b)$	[N]	resistance force to the slip velocity
Fr	[–]	Froude number $Fr = v_w/\sqrt{g l_w}$
g	[m/s^2]	gravitation acceleration
h	[m]	height of fall
h_p	[m]	penetration depth
l_w	[m]	reference length
Δl	[m]	orifice spacing
ΔL	[m]	horizontal distance between orifice and air bubbles at the water surface
$M_{w,z}$	[N]	vertical momentum flux
p	[Pa]	pressure
p_e	[Pa]	subatmospheric pressure
Δp_e	[Pa]	pressure difference
p_{atm}	[Pa]	atmospheric pressure
Q_a	[m^3/s]	air discharge

q_a	$[m^2/s]$	specific flow rate (air) per unit width
Q_{ae}	$[m^3/s]$	total rate of entrained air
q_{ae}	$[m^2/s]$	specific rate of entrained air per unit width
Q_{at}	$[m^3/s]$	total air transport rate
q_{at}	$[m^2/s]$	specific air transport rate per unit width
Q_w	$[m^3/s]$	water discharge
q_w	$[m^2/s]$	specific water discharge per unit width
Re	[–]	Reynolds number $Re = (v_w \cdot l_w/(\mu_w/g))$
Tu	[–]	turbulence characteristics
v_b	[m/s]	bubble rise velocity
v_e	[m/s]	velocity at the line of air entrainment, impingement velocity
v_H	[m/s]	cross flow velocity
v_t	[m/s]	turbulent fluctuations, (RMS)
v'	[m/s]	velocity fluctuation
v_w	[m/s]	water velocity
We	[–]	Weber number $We = v_w/\sqrt{(\sigma_{wa}/\rho_w \cdot l_w)}$
y	[m]	water depth
y_2	[m]	outflow water depth downstream of the hydraulic jump
y_e	[m]	water depth at the point of air entrainment, inflow water depth upstream of the hydraulic jump
Z	[–]	liquid parameter $Z = g\,\mu_w^4/\rho_w\sigma_{wa}^3$
β	[–]	ratio of air discharge to water discharge $\beta = q_a/q_w$
β_e	[–]	relative air entrainment $\beta_e = q_{ae}/q_w$
γ_w	$[kN/m^3]$	specific weight of the liquid (water)
ρ_a	$[kg/m^3]$	density of air
ρ_w	$[kg/m^3]$	density of the liquid (water)
μ_w	[kg/ms]	dynamic viscosity of the liquid (water)
υ_w	$[m^2/s]$	kinematic viscosity of the liquid (water)
σ_{wa}	[N/m]	surface tension at the gas-liquid (air-water) interface